Article

Supramolecular Pattern of Fullerene on 2D Bimolecular "Chessboard" Consisting of Bottom-up Assembly of Porphyrin and Phthalocyanine Molecules

Soichiro Yoshimoto, Yosuke Honda, Osamu Ito, and Kingo Itaya

J. Am. Chem. Soc., **2008**, 130 (3), 1085-1092 • DOI: 10.1021/ja077407p

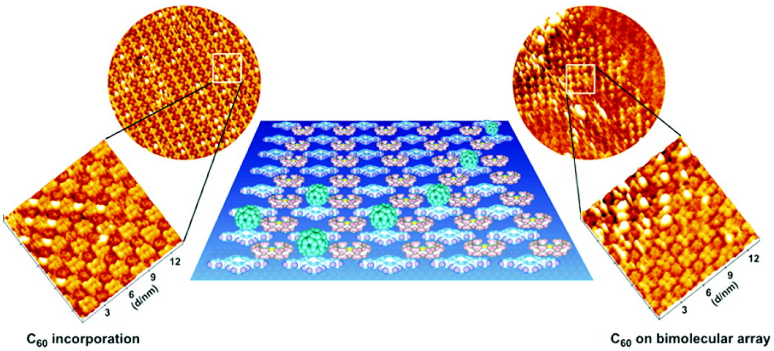

More About This Article

Additional resources and features associated with this article are available within the HTML version:

- Supporting Information
- Links to the 5 articles that cite this article, as of the time of this article download
- Access to high resolution figures
- Links to articles and content related to this article
- Copyright permission to reproduce figures and/or text from this article

View the Full Text HTML

J|A|C|S
ARTICLES
Published on Web 12/29/2007

Supramolecular Pattern of Fullerene on 2D Bimolecular "Chessboard" Consisting of Bottom-up Assembly of Porphyrin and Phthalocyanine Molecules

Soichiro Yoshimoto,*[,†,§] Yosuke Honda,[†] Osamu Ito,[‡] and Kingo Itaya*[,†]

Department of Applied Chemistry, Graduate School of Engineering, Tohoku University, 6-6-07 Aoba, Sendai 980-8579, Japan, and Institute of Multidisciplinary Research for Advanced Materials, Tohoku University, Katahira, Aoba-ku, Sendai 980-8577, Japan

Received September 25, 2007; E-mail: so-yoshimoto@aist.go.jp; itaya@atom.che.tohoku.ac.jp

Abstract: Two-component adlayers consisting of zinc(II) phthalocyanine (ZnPc) and a metalloporphyrin, such as zinc(II) octaethylporphyrin (ZnOEP) or zinc(II) tetraphenylporphyrin (ZnTPP), were prepared by immersing either an Au(111) or Au(100) substrate in a benzene solution containing those molecules. The bimolecular adlayers thus prepared were investigated in 0.1 M $HClO_4$ by cyclic voltammetry (CV) and electrochemical scanning tunneling microscopy (EC-STM). A supramolecularly organized "chessboard" structure was formed for the ZnPc and ZnOEP bimolecular array on Au(111), while characteristic nanohexagons were found in the ZnTPP and ZnOEP bimolecular adlayer. EC-STM revealed that the surface mobility and the molecular re-organization of ZnPc and ZnOEP on Au(111) were tunable by manipulating the electrode potential, whereas the ZnTPP and ZnOEP bimolecular array was independent of the electrode potential. A "bottom-up" hybrid assembly of fullerene molecules was formed successfully on an alternate array of bimolecular ZnPc and ZnOEP molecules. The bimolecular "chessboard" served as a template to form the supramolecular assembly of C_{60} by selective trapping in the open spaces. A supramolecular organization of ZnPc and ZnOEP was also found on the reconstructed Au(100)−(hex) surface. A highly ordered, compositionally disordered but alternate array of ZnPc and ZnOEP was formed on the reconstructed Au(100)−(hex) surface, indicating that the bimolecular adlayer structure is dependent on the atomic arrangement of underlying Au in the formation of supramolecular nanostructures composed of those molecules. On the bimolecular array consisting of ZnPc and ZnOEP on the Au(100)−(hex), no highly ordered supramolecular assembly of C_{60} was found, suggesting that the supramolecular assembly of C_{60} molecules is strongly dependent upon the bimolecular packing arrangement of ZnPc and ZnOEP.

Introduction

Since the establishment of the concept of supramolecular chemistry,[1,2] attempts have been made to fabricate functional devices from simple molecular components mimicking biological systems.[3] For example, porphyrin-fullerene and phthalocyanine-fullerene supramolecular assemblies have been extensively studied because of the interest in photoinduced energy and electron-transfer processes for photonics and solar cells.[4−8] Supramolecular organizations based on noncovalent interactions, such as hydrogen bonding,[9−11] dipole coupling,[12,13] metal-organic coordination,[14,15] and intermolecular DNA recognition,[16,17] have also been explored to control surface properties and to construct two-dimensional (2D) nanoarchitectures on

[†] Department of Applied Chemistry, Graduate School of Engineering, Tohoku University.

[‡] Institute of Multidisciplinary Research for Advanced Materials, Tohoku University.

[§] Present address: National Institute of Advanced Industrial Science and Technology (AIST), Central 6, 1−1−1 Higashi, Tsukuba, Ibaraki 305-8566, Japan.

(1) Lehn J. M. *Supramolecular Chemistry*; Wiley-VCH: Weinheim, 1995.
(2) (a) Lehn, J. M. *Science* **2002**, *295*, 2400. (b) Lehn, J. M. *Chem. Soc. Rev.* **2007**, *36*, 151.
(3) Gust, D.; Moore, T. A.; Moore, A. L. *Acc. Chem. Res.* **2001**, *34*, 40.
(4) Kim, D.; Osuka, A. *J. Phys. Chem. A* **2003**, *107*, 8791.
(5) Guldi, D. M. *Chem. Soc. Rev.* **2002**, *31*, 22.
(6) El-Khouly, M. E.; Ito, O.; Smith, P. M.; D'Souza, F. *J. Photochem. Photobiol. C* **2004**, *5*, 79.
(7) Imahori, H.; Fukuzumi, S. *Adv. Funct. Mater.* **2004**, *14*, 525.
(8) Boyd, P. D. W.; Reed, C. A. *Acc. Chem. Res.* **2005**, *38*, 235.
(9) De Feyter, S.; De Schryver, F. C. *J. Phys. Chem. B* **2005**, *109*, 4290.
(10) (a) Theobald, J. A.; Oxtoby, N. S.; Phillips, M. A.; Champness, N. R.; Beton, P. H. *Nature* **2003**, *424*, 1029. (b) Theobald, J. A.; Oxtoby, N. S.; Champness, N. R.; Beton, P. H.; Dennis, T. J. S. *Langmuir* **2005**, *21*, 2038. (c) Perdigão, L. M. A.; Perkins, E. W.; Ma, J.; Staniec, P. A.; Rogers, B. L.; Champness, N. R.; Beton, P. H. *J. Phys. Chem. B* **2006**, *110*, 12539.
(11) Griessl, S. J. H.; Lackinger, M.; Jamitzky, F.; Markert, T.; Hietschold, M.; Heckl, W. M. *J. Phys. Chem. B* **2004**, *108*, 11556.
(12) (a) Yokoyama, T.; Kamikado, T.; Yokoyama, S.; Mashiko, S. *J. Chem. Phys.* **2004**, *121*, 11993. (b) Yokoyama, T.; Yokoyama, S.; Kamikado, T.; Okuno, Y.; Mashiko, S. *Nature* **2001**, *413*, 619.
(13) (a) Spillmann, H.; Kiebele, A.; Stöhr, M.; Jung, T. A.; Bonifazi, D.; Cheng, F.; Diederich, F. *Adv. Mater.* **2006**, *18*, 275. (b) Bonifazi, D.; Kiebele, A.; Stöhr, M.; Cheng, F.-Y.; Jung, T. A.; Diederich, F.; Spillmann, H. *Adv. Funct. Mater.* **2007**, *17*, 1051.
(14) (a) Barth, J. V.; Costantini, G.; Kern, K. *Nature* **2005**, *437*, 671, and references therein. For example, (b) Stepanow, S.; Lingenfelder, M.; Dmitriev, A.; Spillmann, H.; Delvigne, E.; Lin, N.; Deng, X.; Cai, C.; Barth, J. V.; Kern, K. *Nat. Mater.* **2004**, *3*, 229. (c) Stepanow, S.; Lin, N.; Barth, J. V.; Kern, K. *Chem. Commun.* **2006**, 2153.
(15) Zhang, H.-M.; Zhao, W.; Xie, Z.-X.; Long, L.-S.; Mao, B.-W.; Xu, X.; Zheng, L.-S. *J. Phys. Chem. C* **2007**, *111*, 7570.
(16) Rothemund, P. W. K. *Nature* **2006**, *440*, 297.
(17) (a) Park, S.-H.; Pistol, C.; Ahn, S. J.; Reif, J. H.; Lebeck, A. R.; Dwyer, C.; LaBean, T. H. *Angew. Chem., Int. Ed.* **2006**, *45*, 735. (b) Chhabra, R.; Sharma, J.; Ke, Y.; Liu, Y.; Rinker, S.; Lindsay, S.; Yan, H. *J. Am. Chem. Soc.* **2007**, *129*, 10304.

solid surfaces.[18−22] The "bottom-up" supramolecular assembly strategy is an attractive and promising approach for the construction of nanoarchitectures. However, the preparation of high-quality composite thin films based on the bottom-up approach requires an understanding of the relationship between adlayer structure and function at the nanoscale.[13b,14,18,19] To relate the structure with the function, it is important to understand the effect of the bicomponent arrays with different physical and chemical properties on the formation of the bottom-up molecular assembly.

One attractive "bottom-up" method is to prepare binary and hybrid nanostructures on a solid surface by supramolecular assembly of organic functional materials and to demonstrate specific functions, such as catalysis, photoinduced electron transfer, and conductivity derived from the formation of various nanostructures. Specific optical properties, such as light-emission and light absorption of porphyrin tape,[20] nanoprism,[21] and nanosheets,[22] are expected to result from controlled nanoarchitectures. Especially, fullerenes are considered to be suitable building blocks for three-dimensional molecular architectures owing to their strong π-electron accepting ability.[23,24] If 2D-ordered arrays consisting of porphyrin and phthalocyanine can be patterned on a solid surface, 3D-supramolecular assembled layers of C_{60} on the 2D-patterned surface will produce photo-induced conductive nanodots or optical nanowires because the excitation wavelength of porphyrin is different from that of phthalocyanine.[6]

Scanning tunneling microscopy (STM) has been used to understand and design two-dimensional nanoarrays by bottom-up assembly.[14,18,19] The formation of mixed molecular adlayers consisting of two or three components has been attempted extensively by using vapor and wet deposition techniques.[9−15,25−28] In particular, the report on the two-component array of phthalocyanine and porphyrin by Hipps and co-workers encouraged us to investigate bimolecular adlayers prepared by wet deposition.[25a] Since our first report on the hydrophobic cobalt(II) teteraphenylporphyrin (CoTPP) adlayer prepared from benzene solution,[29] we have investigated and clarified important factors determining molecular assemblies of various porphyrins and phthalocyanines at electrode surfaces.[26,30] The formation of characteristic two-dimensional arrays is controlled by chemical structure, central metal ion, crystallographic orientation (underlying Au atomic arrangement), and potential manipulation.[19,26,30] A unique and precise control of 2D molecular assemblies is of great interest for exploring further applications. For example, the formation of a 2D supramolecular nanoporous network using hydrogen bonding[10] or metal-organic coordination[14b] has been reported. The supramolecular network arrays can distinguish between C_{60} and C_{84} molecules as guest molecules. We succeeded in forming a 1:1 supramolecular assembly consisting of fullerenes such as C_{60}, open-cage C_{60} derivative, and ferrocene-linked C_{60}, and metalloporphyrins such as zinc(II) octaethylporphyrin (ZnOEP)[31a−31d] and nickel(II) octaethylporphyrin (NiOEP)[31e] on both Au(111) and Au(100) surfaces. Such a supramolecular assembly produced through donor−acceptor interaction improves electrochemical performances by the control of molecular orientation.[19,31] Furthermore, very recently, Stöhr and Jung's group reported "supramolecular bearing" through piece-by-piece assembly of weakly aggregated ZnOEP−C_{60} complex trapped in the hexagonal molecular network forming hydrogen bonding among 4,9-diaminoperylenequinone-3,10-diimine (DPDI) molecules on Cu(111) in UHV.[32] Thus, the knowledge on the formation of bifunctional array consisting of porphyrin and phthalocyanine should be extendable to the supramolecular nanodevices based on the layer-by-layer growth at heterogeneous interfaces.

In the present paper, we propose a guide for designing two-dimensional (2D) alternate arrays consisting of bicomponents and for producing patterns of fullerene nanodots on surface-supported supramolecular nanostructures from solution phase. The formation of supramolecularly patterned fullerenes on the 2D bimolecular structure consisting of porphyrin and phthalocyanine molecules was investigated on Au(111) and Au(100) electrode surfaces by using electrochemical scanning tunneling microscopy (EC-STM).

Experimental Section

Fullerene (C_{60}) was purchased from MER Corp. (purity ≥99.98%). Zinc(II) phthalocyanine (ZnPc), 5,10,15,20-tetraphenyl-21*H*,23*H*-porphine zinc(II) (ZnTPP), and 2,3,7,8,12,13,17,18-octaethyl-21*H*,23*H*-porphine zinc(II) (ZnOEP) were purchased from Aldrich and used without further purification. Benzene was obtained from Kanto Chemical Co. (spectroscopy grade).

Au(111) and Au(100) single-crystal electrodes were prepared by the methods described in our previous papers.[19a,24,26] Adlayers of ZnOEP

(18) De Feyter, S.; De Schryver, F. C. *Chem. Soc. Rev.* **2003**, *32*, 139.
(19) (a) Itaya, K. *Prog. Surf. Sci*. **1998**, *58*, 121. (b) Yoshimoto, S. *Bull. Chem. Soc. Jpn.* **2006**, *79*, 1167. (c) Yoshimoto, S.; Itaya, K. *J. Porphyrins Phthalocyanines* **2007**, *11*, 313.
(20) Tsuda, A.; Osuka, A. *Science* **2001**, *293*, 79.
(21) Hu, J.-S.; Guo, Y.-G.; Liang, H.-P.; Wan, L.-J.; Jiang, L. *J. Am. Chem. Soc.* **2005**, *127*, 17090.
(22) Wang, Z.; Li, Z.; Medforth, C. J.; Shelnutt, J. A. *J. Am. Chem. Soc.* **2007**, *129*, 2440.
(23) (a) Néel, N.; Kröger, J.; Berndt, R. *Adv. Mater*. **2006**, *18*, 174. (b) Xiao, W.; Ruffieux, P.; Aït-Mansour, K.; Gröning, O.; Palotas, K.; Hofer, W. A.; Gröning, P.; Fasel, R. *J. Phys. Chem. B* **2006**, *110*, 21394.
(24) Yoshimoto, S.; Tsutsumi, E.; Narita, R.; Murata, Y.; Murata, M.; Fujiwara, K.; Komatsu, K.; Ito, O.; Itaya, K. *J. Am. Chem. Soc.* **2007**, *129*, 4366.
(25) (a) Hipps, K. W.; Scudiero, L.; Barlow, D. E.; Cooke, M. P., Jr. *J. Am. Chem. Soc.* **2002**, *124*, 2126. (b) Scudiero, L.; Hipps, K. W.; Barlow, D. E. *J. Phys. Chem. B* **2003**, *107*, 2903. (c) Barlow, D. E.; Scudiero, L.; Hipps, K. W. *Langmuir* **2004**, *20*, 4413.
(26) (a) Yoshimoto, S.; Higa, N.; Itaya, K. *J. Am. Chem. Soc.* **2004**, *126*, 8540. (b) Suto, K.; Yoshimoto, S.; Itaya, K. *J. Am. Chem. Soc.* **2003**, *125*, 14976. (c) Suto, K.; Yoshimoto, S.; Itaya, K. *Langmuir* **2006**, *22*, 10766.
(27) (a) Yang, Z.-Y.; Lei, S.-B.; Gan, L.-H.; Wan, L.-J.; Wang, C.; Bai, C.-L. *ChemPhysChem* **2005**, *6*, 65. (b) Lu, J.; Lei, S.-B.; Zeng, Q. D.; Kang, S. Z.; Wang, C.; Wan, L.-J.; Bai, C. L. *J. Phys. Chem. B* **2004**, *108*, 5161. (c) Xu, L. P.; Yan, C. J.; Wan, L.-J.; Jiang, S. G.; Liu, M. H. *J. Phys. Chem. B* **2005**, *109*, 14773. (d) Kong, X.-H.; Deng, K.; Yang, Y.-L.; Zeng, Q.-D.; Wang, C. *J. Phys. Chem. C* **2007**, *111*, 9235.
(28) Barrena, E.; de Oteyza, D. G.; Dosch, H.; Wakayama, Y. *ChemPhysChem* **2007**, *8*, 1915.
(29) Yoshimoto, S.; Tada, A.; Suto, K.; Narita, R.; Itaya, K. *Langmuir* **2003**, *19*, 672.
(30) (a) Yoshimoto, S.; Tada, A.; Suto, K.; Itaya, K. *J. Phys. Chem. B* **2003**, *107*, 5836. (b) Yoshimoto, S.; Suto, K.; Itaya, K.; Kobayashi, N. *Chem. Commun.* **2003**, 2174. (c) Yoshimoto, S.; Inukai, J.; Tada, A.; Abe, T.; Morimoto, T.; Osuka, A.; Furuta, H.; Itaya, K. *J. Phys. Chem. B* **2004**, *108*, 1948. (d) Yoshimoto, S.; Tada, A.; Itaya, K. *J. Phys. Chem. B* **2004**, *108*, 5171. (e) Yoshimoto, S.; Suto, K.; Tada, A.; Kobayashi, N.; Itaya, K. *J. Am. Chem. Soc.* **2004**, *126*, 8020. (f) Yoshimoto, S.; Tsutsumi, E.; Suto, K.; Honda, Y.; Itaya, K. *Chem. Phys.* **2005**, *319*, 147. (g) Yoshimoto, S.; Yokoo, N.; Fukuda, T.; Kobayashi, N.; Itaya, K. *Chem. Commun.* **2006**, 500. (h) Yoshimoto, S.; Sato, K.; Sugawara, S.; Chen, Y.; Ito, O.; Sawaguchi, T.; Niwa, O.; Itaya, K. *Langmuir* **2007**, *23*, 809. (i) Yoshimoto, S.; Sawaguchi, T.; Su, W.; Jiang, J.; Kobayashi, N. *Angew. Chem., Int. Ed.* **2007**, *46*, 1071.
(31) (a) Yoshimoto, S.; Tsutsumi, E.; Honda, Y.; Ito, O.; Itaya, K. *Chem. Lett.* **2004**, *33*, 914. (b) Yoshimoto, S.; Tsutsumi, E.; Honda, Y.; Murata, Y.; Murata, M.; Komatsu, K.; Ito, O.; Itaya, K. *Angew. Chem., Int. Ed.* **2004**, *43*, 3044. (c) Yoshimoto, S.; Honda, Y.; Murata, Y.; Murata, M.; Komatsu, K.; Ito, O.; Itaya, K. *J. Phys. Chem. B* **2005**, *109*, 8547. (d) Yoshimoto, S.; Saito, A.; Tsutsumi, E.; D'Souza, F.; Ito, O.; Itaya, K. *Langmuir* **2004**, *20*, 11046. (e) Yoshimoto, S.; Sugawara, S.; Itaya, K. *Electrochemistry* **2006**, *74*, 175.
(32) Stöhr, M.; Wahl, M.; Spillmann, H.; Gade, L. H.; Jung, T. A. *Small* **2007**, *3*, 1336.

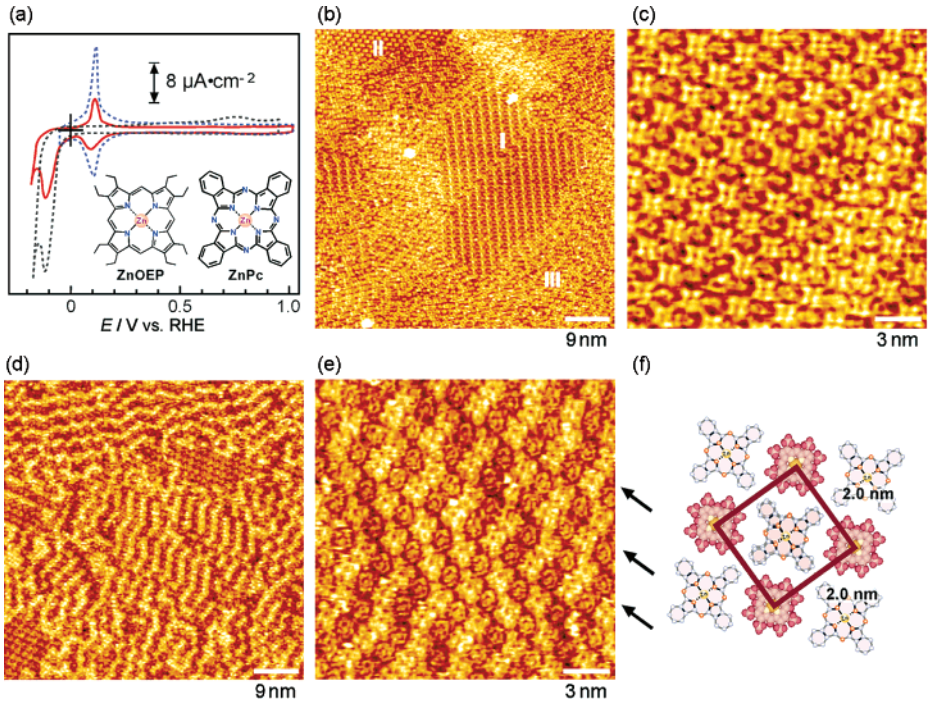

Figure 1. (a) Cyclic voltammograms recorded at a scan rate of 50 mV s^{-1}. The red solid line was obtained with a bimolecular ZnPc and ZnOEP-modified Au(111) electrode. The blue and black dotted lines were obtained with Au(111) electrodes individually modified with ZnPc and ZnOEP, respectively. (b-e) STM images obtained at (b) 0.78 V, (c) 0.60 V, (d and e) 0.80 V vs RHE, respectively. Tip potentials and tunneling currents were 0.40 V vs RHE and 1.00 nA for panel (b), 0.16 V vs RHE and 0.60 nA for panel (c), and 0.45 V vs RHE and 1.25 nA for panels (d) and (e), respectively. (f) Proposed model of bimolecular chessboard consisting of ZnPc and ZnOEP on the Au(111) surface.

and ZnPc binary arrays were formed by immersing either Au(111) or Au(100) substrate for 10−30 s into a saturated ZnPc benzene solution containing ∼1−3 μM ZnOEP or into an ∼100 μM ZnTPP benzene solution containing ∼1 μM ZnOEP. Prior to the immersion, the Au(111) substrate was annealed in hydrogen flame and cooled down in a clean bench for 3 min to avoid contamination.[24,26] The modified Au(111) substrate was then immersed into an ∼1−5 μM C_{60} benzene solution for less than 5 s. The Au(111) substrate with a C_{60} array on the bimolecular ZnPc and ZnOEP adlayer thus produced was rinsed with ultrapure water and transferred into an electrochemical STM cell filled with 0.1 M $HClO_4$ (Cica-Merck, ultrapure grade).

Electrochemical STM measurements were performed in 0.1 M $HClO_4$ by using a Nanoscope E system (Digital Instruments, Santa Barbara) with a tungsten tip etched in 1 M KOH. To minimize residual faradaic currents, tips were coated with either nail polish or polyethylene. STM images were obtained in the constant-current mode with a high-resolution scanner (HD-0.5I). All potential values (both substrate and tip) are referred to the reversible hydrogen electrode (RHE).

Results and Discussion

Formation of Supramolecularly Organized Bimolecular ''Chessboard''. Figure 1a shows cyclic voltammograms of ZnPc and ZnOEP-modified Au(111) electrodes in 0.1 M $HClO_4$. Results reported in our previous papers indicated that ZnPc- and ZnOEP-modified Au(111) electrodes undergo phase transition and desorption at 0.10 V and −0.05 V, respectively (black and blue dotted lines).[30f,31a] By comparing the current density on the CV for the Au(111) electrode modified with a mixture of ZnPc and ZnOEP with that for the electrode modified separately with either ZnPc or ZOEP, the ratio in number of ZnPc to ZnOEP molecules present on the Au(111) surface was roughly estimated to be equal to unity. After the CV profiles were confirmed, in situ STM measurements were performed in 0.1 M $HClO_4$. Figure 1b shows a typical large-scale STM image of bifunctional ZnPc and ZnOEP arrays on Au(111) obtained at an open circuit potential (OCP), which was approximately equal to 0.80 V. The terrace was entirely covered with ZnPc and ZnOEP molecules with the ratio nearly equal to 1:1, i.e., the adlayer was composed of three different regions: (1) a well-ordered ZnPc and ZnOEP mixed region I, (2) a pure ZnOEP region II, and (3) a compositionally disordered region III. These adlayers were formed on the reconstructed Au(111) surface, probably due to the donation of π-electrons of both ZnPc and ZnOEP molecules to the Au(111) surface, i.e., the Au surface becomes negatively charged upon adsorption of ZnPc and ZnOEP. Such phenomena have been observed at single component adlayers of ZnOEP,[31a,31d] ZnPc,[30f] and coronene.[24] Further details of the internal structure, orientation, and packing arrangement in region I are seen in the close-up view shown in Figure 1c, which reveals that an alternate molecular arrangement is present uniformly on Au(111). The arrangement of ZnPc and ZnOEP resembles a "chessboard" in appearance. Individual ZnPc molecules are propeller-shaped with a dark spot at the center and four additional spots at the corners, whereas each ZnOEP molecule in the dark row is in the shape of a doughnut with several additional spots. In this domain, the image of each ZnPc molecule is more enhanced in contrast compared to that of ZnOEP, suggesting that the electronic state of ZnPc is different from that of ZnOEP in the bimolecular chessboard structure. These molecular shapes of ZnPc and ZnOEP have already been identified by high-resolution STM imaging in our previous papers.[30f,31d] According to a recent paper on ZnOEP and DPDI systems in UHV, the rotation of ZnOEP molecules in the hexagonal molecular network consisting of DPDI on Cu(111) is controlled by bias voltage and tunneling current at

temperatures lower than 77 K.[33] On the basis of the STM images, it is judged that each ZnOEP molecule surrounded by four ZnPc molecules does not rotate in the bimolecular chessboard. The intermolecular distance between ZnPc (or ZnOEP) molecules was measured to be approximately 2.0 nm. The adlattice is in the shape of a square with one ZnOEP molecule surrounded by four ZnPc molecules. Although the bimolecular chessboard structure was predominantly formed under the present experimental conditions, ZnPc molecular rows arranged in zigzag fashion were also found on the terrace, as shown in Figure 1d. The close-up view in Figure 1e reveals that each set of two molecules of either ZnPc or ZnOEP is arranged alternately, as indicated by the arrow signs. When the modification condition was slightly changed by assembling in a 1:3 mixed solution for 30 s on an Au(111) surface, highly ordered ZnOEP domains were dominantly observed on a terrace, indicating that the organization of ZnOEP molecules is more stable than that of ZnPc molecules on Au(111). This finding suggests that the formation of chessboard or zigzag structure depends on the concentrations and the component ratio of the mixed solution. The appearance of the chessboard domain remained unchanged when the potential was manipulated between 0.85 and 0.15 V. In region II, the single component domain consisting of ZnOEP was stable in the potential range between 1.00 and 0 V, as described in our previous paper.[31a] It should be noted that the observed adlayers in air were identical to those obtained at potentials near OCP in the aqueous solution when STM measurements of the "as-prepared" adlayer were performed under ambient conditions. We believe that the as-prepared adlayers remain thermodynamically stable in both air and aqueous solution at or near OCP.

In contrast, a structural change was observed in region III, when the potential was held at various constant values. Figure 2, parts a−e, shows the potential-dependent STM images of region III. In Figure 2a, the terrace was covered with several small ordered domains consisting of ZnPc and ZnOEP. At 0.60 V, stripes of alternately arranged molecular rows were present predominantly on the terrace, as shown in Figure 2b. The high-resolution STM image of Figure 2c shows that two of the four benzene rings in each ZnPc molecule fit into the space between neighboring ZnPc molecules in the ZnPc molecular row. The intermolecular distance between ZnPc (or ZnOEP) molecules in each molecular row was found to be 1.45 nm, whereas the periodic spacing between two ZnPc (or ZnOEP) molecular rows was approximately 3.0 nm. The formation of the stripes was also dependent on the time of image recording (see Figure S1 of the Supporting Information). The formation of stripes was accelerated in region III by potential manipulation. At 0.15 V, the STM image became unclear, and several domains consisting of ZnOEP molecules only were immediately formed on the terrace, as shown in Figure 2d. ZnPc molecules were highly mobile on the surface because of the electrochemical phase transition,[30f] whereas the pure ZnOEP adlayer was stable even at or near this potential.[31a] However, when the electrode potential was returned by stepping from 0.15 V to a value more positive than 0.20 V, ZnPc domains began to appear on the terrace. The squarely and hexagonally arranged regions in Figure 2e were composed of ZnPc and ZnOEP molecules, respectively. Thus,

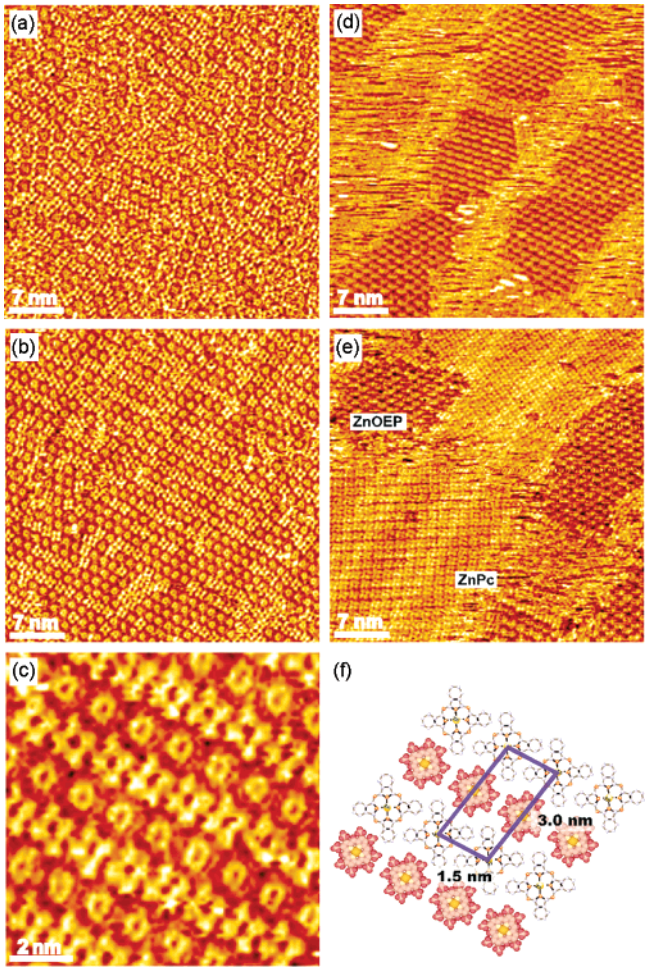

Figure 2. Potential-dependent STM images (40 × 40 nm^2) of bimolecular ZnPc and ZnOEP array on Au(111) in 0.1 M $HClO_4$ obtained at (a) 0.60 V, (b) 0.44 V, (c) 0.53 V, (d) 0.15 V, and (e) 0.60 V vs RHE. (c) A close-up view (10 × 10 nm^2) of (b). Tip potentials and tunneling currents were 0.20 V and 1.78 nA for panel (a), 0.19 V and 0.66 nA for panel (b), 0.19 V and 0.52 nA for panel (c), 0.38 V and 1.30 nA for panel (d), and 0.38 V and 1.00 nA for panel (e), respectively. (f) Proposed model of alternately arranged ZnPc and ZnOEP array on Au(111) surface.

ZnPc molecules can be selectively desorbed from the surface, whereas ZnOEP molecules take place to assemble each other on the surface by the potential manipulation. Electrochemical potential manipulation caused a similar phase separation in the CoPc and CuOEP mixed array on Au(111).[26a,26c] The present results indicate that the electrochemical phase separation was caused by the difference in scaffold between Pc and OEP, *not* by the difference in central metal ion. However, the adlayer structures observed in the present study were different from those of the CoPc and CuOEP system.[26a] One possible reason for this difference is that central metal ions play a significant role in the formation of the characteristic chessboard, i.e., the π-electron donating ability in the 2D supramolecular assembly, which brings about a weak and subtle interaction such as van der Waals interaction, may depend on the central metal ions. The phase-separated domains were stable when the potential was returned to 0.60 V, i.e., the bimolecular chessboard is a meta-stable adlayer formed during the modification. Therefore, the surface charge density at the electrochemical interface appears to contribute not only to the molecule−substrate interaction but also to the interaction between the molecules.

(33) Wahl, M.; Stöhr, M.; Spillmann, H.; Jung, T. A.; Gade, L. H. *Chem. Commun.* **2007**, 1349.

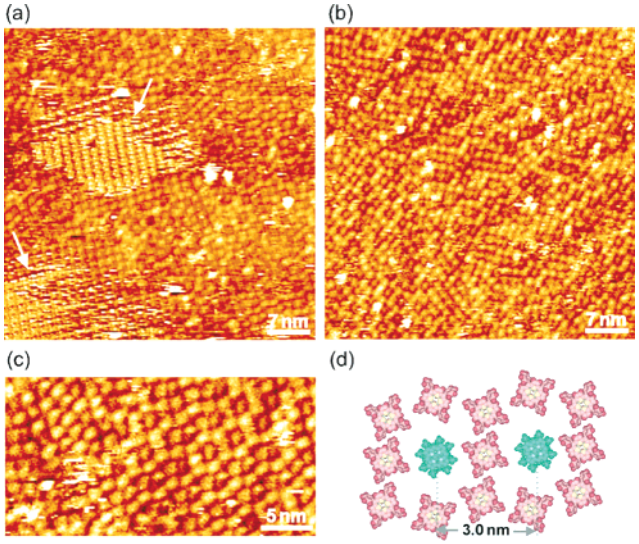

Figure 3. (a and b) Large-scale (50 × 50 nm^2) and (c) high-resolution (15 × 30 nm^2) STM images of ZnTPP and ZnOEP bimolecular array on Au(111) obtained at 0.80 V vs RHE in 0.1 M $HClO_4$. Tip potential and tunneling current were 0.27 V and 0.54 nA for panel (a) and 0.27 V and 0.85 nA for (b) and (c). (d) Proposed model of nanohexagon consisting of ZnTPP and ZnOEP.

To examine and understand the effect of the chemical structure on the formation of bimolecular array, ZnTPP which has rotational phenyl moieties was mixed with ZnOEP, and the formation of the bimolecular array was examined on Au(111). In this case, ZnTPP molecules often formed its bilayer, as can be seen in Figure 3a. The brighter parts with square packing arrangement indicate bilayer formation of ZnTPP molecules, as marked by the white arrows. As reported in our previous paper, ZnTPP molecules easily form a multilayer on Au(111) in benzene solution.[30f] ZnTPP has an attractive intermolecular interaction perpendicular to the molecular plane, which is derived from the characteristic property of ZnTPP. A large, positive charge in the central cavity such as zinc ion of the porphyrin π-system leads to a favorable interaction with π-electrons of the pyrrole of the neighboring porphyrin.[34] In contrast, several parts showing squarely arranged ZnTPP domains and disordered regions consisting of ZnTPP and ZnOEP are seen in the first layer. Increasing the tunneling current made it possible to observe the first adlayer consisting of ZnTPP and ZnOEP. When the tunneling current was increased up to 0.85 nA, a clearer first adlayer consisting of ZnTPP and ZnOEP appeared on the terrace. In Figure 3b, several zigzag patterns can be seen as brighter spots. Characteristic nanostructures with a dark spot in each bright nanohexagon, were found in the bimolecular array on Au(111). On the basis of the observed ratio of ZnTPP to ZnOEP in number, it is assumed that the bright spot is ZnTPP, whereas the dark spot is ZnOEP. The result suggests that the electronic structure is different between ZnTPP and ZnOEP molecules in the bimolecular array. Thus, ZnTPP and ZnOEP molecules can be distinguished based on image contrast. From the STM image shown in Figure 3b, it seems that each ZnOEP molecule is separated from ZnTPP molecules. A high-resolution STM image of ZnTPP and ZnOEP is shown in Figure 3c. Although we failed to obtain a high-quality molecular resolution image with distinct molecular shapes, it can be seen that one ZnOEP molecule (dark image) is surrounded by eight ZnTPP molecules. The intermolecular distance between the nearest ZnOEP molecules in nanohexagon cavity is measured to be 2.8−3.0 nm, which is slightly greater than the hexagonal molecular network consisting of the DPDI system reported by Stöhr et al.[32] On the basis of the cavity size and the intermolecular distance, a structural model of nanohexagon is proposed in Figure 3d. It is assumed that a ZnOEP molecule is positioned at the center surrounded hexagonally by eight ZnTPP molecules. The adlayer was stable at or near 0.10 V, i.e., no structural change occurred in the ZnTPP and ZnOEP mixed system. The intermolecular interaction between adjacent ZnTPP molecules is stronger than that between ZnPc molecules, because the phenyl moieties between adjacent ZnTPP molecules can attract each other through $\pi-\pi$ interaction. Actually, the single component adlayer of ZnTPP and that of ZnOEP are more stable than that of ZnPc adlayer against potential manipulation.[30f]

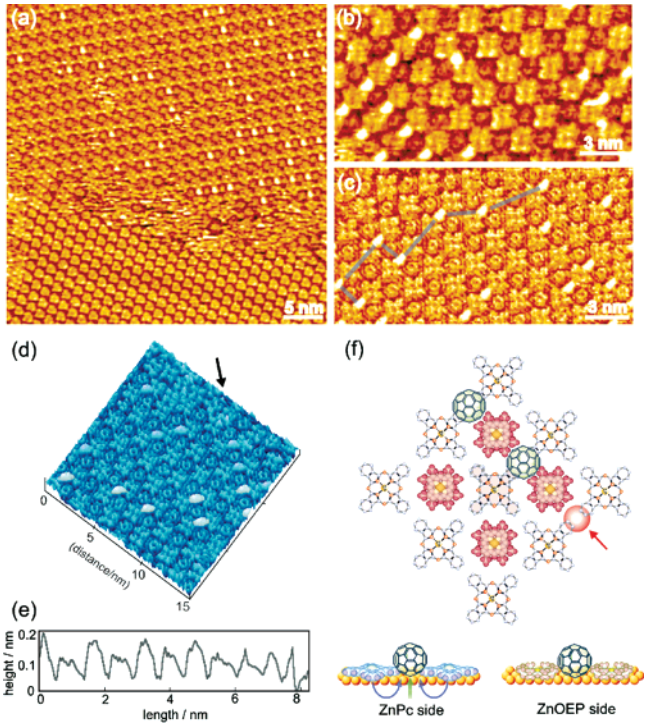

Figure 4. (a) STM image (40 × 40 nm^2) of C_{60} array in the bimolecular chessboard consisting of ZnPc and ZnOEP on Au(111) obtained at 0.75 V vs RHE in 0.1 M $HClO_4$. Tip potential and tunneling current were 0.27 V and 0.41 nA. (b and c) STM images (10 × 20 nm^2) obtained at (b) 0.60 V and (c) 0.67 V vs RHE. Tip potential and tunneling current were 0.27 V and 0.74 nA for panel (b) and 0.23 V and 0.68 nA for panel (c). (d) Height-shaded view of (c). (e) The cross-sectional profile aligned in the direction of the arrow. (f) Proposed models for top and side views of C_{60} array in bimolecular chessboard.

Selective Supramolecular Assembly of Fullerene. The characteristic formation of C_{60} supramolecular assembly took place on the bimolecular chessboard because the adlayer was stable with respect to potential manipulation. Figure 4a shows an STM image of the bimolecular chessboard on Au(111) at a low coverage of C_{60}. Interestingly, many bright spots were found in the bimolecular chessboard (see also Figure S2 of the Supporting Information), whereas no such bright spots were observed in the pure ZnOEP domain (the lower portion of Figure 4a). The result demonstrates that the electronic state of ZnOEP in the bimolecular chessboard is quite different from that of

(34) Hunter, C. A.; Sanders, J. K. M. *J. Am. Chem. Soc.* **1990**, *112*, 5525.

pure ZnOEP domain. Further careful inspection revealed that the incorporation of individual C_{60} molecules into the bimolecular chessboard structure appears to be not uniform. One possibility is that the strength of electron donation at the gap site is different at different locations, because the bimolecular adlayer with the so-called "herringbone" structure is formed at both fcc and hcp sites on the reconstructed Au(111) surface. A close-up view is shown in Figure 4b. Remarkably, each C_{60} molecule is located at the "gap" site between ZnPc molecules, *not* at the center of each ZnPc or ZnOEP molecule, suggesting that the electronic charge distribution on exposed Au (gap) sites is locally enhanced by the formation of the bimolecular chessboard because of the adsorption of those molecules which have π-electron donating ability. According to the recent report on the high-index plane of Au by Xiao et al.,[23b] a C_{60} regular nanochain lattice forms on a vicinal Au(11 12 12) surface with a {111} microfaceted step. Their result indicates that C_{60} molecules adsorb preferentially in the electron-rich regions near the step edges. In the present case, the C_{60} molecules might also adsorb preferentially on bare Au sites rather than on topmost sites of ZnPc or ZnOEP, because the adsorption energy of C_{60} on Au(111) is high, which has been estimated to be 40−60 kcal mol^{-1}.[35] In addition, the C_{60} molecule has a strong electron-accepting ability. The amount of transferred charge estimated from photoemission is 0.8 electron per C_{60} molecule on Au(111).[36] The C_{60} molecule favors the narrow Au site between two neighboring ZnPc molecules. Indeed, each C_{60} molecule in the bimolecular chessboard yields a semi "triangle-shaped" image, *not* a round spot, as shown in Figure 4, parts b and c. As can be seen in Figure 4d, the ZnPc and ZnOEP molecules in the bimolecular chessboard array are separately and clearly imaged, reminiscent of the chemical structure, whereas individual C_{60} molecules appear elliptic in shape. This is not due to a distortion effect during the scan. The height value of each bright spot was measured to be approximately 0.15 nm from the cross-sectional profile aligned in the direction of the arrow in Figure 4e. In general, each C_{60} molecule in the adlayer on Au(111) appears as a round spot because of its rotational motion. It was reported that the electronic structure was observed as an internal structure at the low temperature of 4.5 K in UHV only when the rotational movement of C_{60} on Au(110) was hindered,[37] whereas featureless round spots were observed at room temperature. Therefore, this electronic feature strongly suggests that the bimolecular chessboard consisting of ZnPc and ZnOEP molecules apparently plays a role in the special π-electron donation from the Au surface as a template. As can be seen in the models for top and side views in Figure 4f, the exposed Au (gap) site between ZnPc (or ZnOEP) molecules marked by the red circle pointed at by the arrow sign seems to be locally enhanced. A similar phenomenon was found in the molecular assembly of C_{60} on the coronene-modified Au(111) surface.[24] In addition, Yokoyama and co-workers reported that linear C_{60} arrays were found in the supramolecular wires consisting of 5,15-bis(4-carboxyphenyl)-10,20-bis(3,5-di-*t*-butylphenyl)porphyrin (*trans*-BCaTBPP) molecules on Au(111) in UHV.[38] High-resolution STM images revealed that each C_{60} molecule was located on an open nanopore formed by *trans*-BCaTBPP molecules, *not* at the center of each *trans*-BCaTBPP molecule, implying that the nanopores result from the strong electron accepting ability of fullerene, i.e., fullerene molecules are favorably adsorbed at electron-rich sites. Thus, the bimolecular "chessboard" template can provide a special pattern of C_{60} molecules. As shown in Figures 4c and 4d, a nanosized "great dipper" was found in the bimolecular chessboard.

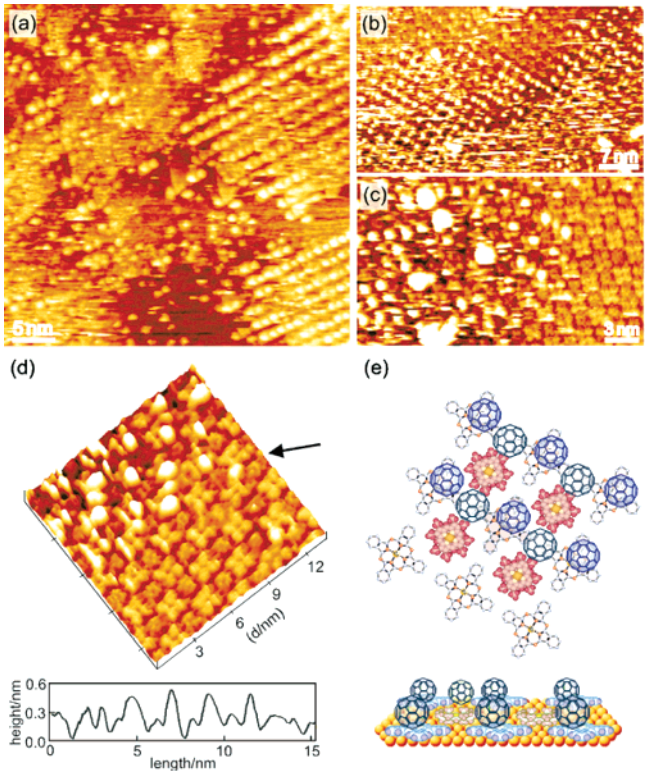

Figure 5. (a and b) Large-scale (40×40 nm^2 for (a) and 30×50 nm^2 for (b)) and (c) high-resolution (15×25 nm^2) STM images of supramolecularly assembled C_{60} molecules on the chessboard structure of ZnPc and ZnOEP on Au(111) obtained at 0.83 V vs RHE in 0.1 M $HClO_4$, respectively. Tip potential and tunneling current were 0.27 V vs RHE and 0.24 nA. (d) Height-shaded view of (c) and the cross-sectional profile aligned in the direction of the arrow. (e) Proposed model of supramolecularly assembled C_{60} molecules on the bimolecular chessboard.

In contrast, when additional C_{60} molecules were deposited on the bimolecular chessboard, squarely arranged C_{60} arrays were formed, as shown in Figure 5a. However, displacement or disturbance of the bimolecular adlayer by C_{60} molecules was often found to take place as shown in Figure 5a (and Figure S3 of the Supporting Information). Although squarely arranged bright spots are clearly visible on the right half of Figure 5a, the remaining regions are disordered. When the size of bimolecular chessboard structure formed on the terrace was large (more than 50 nm^2), supramolecularly assembled C_{60} molecules were found on the bimolecular chessboard. Characteristics of squarely arranged C_{60} molecules were strongly influenced by bias and tunneling conditions. Under the bias condition of 0.56 V with 0.24 nA, the topmost C_{60} layer was easily removed by operating the scanning tip, suggesting that the interaction

(35) Pérez-Jiménez, Á. J.; Palacios, J. J.; Louis, E.; SanFabián, E.; Vergés, J. A. *ChemPhysChem* **2003**, *4*, 388.
(36) Tzeng, C.-T.; Lo, W.-S.; Yuh, J.-Y.; Chu, R.-Y.; Tsuei, K.-D. *Phys. Rev. B* **2000**, *61*, 2263.
(37) Gaisch, R.; Berndt, R.; Gimzewski, J. K.; Reihl, B.; Schlitteler, R. R.; Schneider, W. D.; Tschudy, M. *Appl. Phys. A* **1993**, *57*, 207.
(38) Nishiyama, F.; Yokoyama, T.; Kamikado, T.; Yokoyama, S.; Mashiko, S.; Sakaguchi, K.; Kikuchi, K. *Adv. Mater.* **2007**, *19*, 117.

between C_{60} and the bimolecular chessboard is quite weak. As can be seen in Figure 5b, both the topmost C_{60} molecules and the underlying bimolecular chessboard were clearly visible after several scans. The height-shaded view reproduced in Figure 5c shows that an individual C_{60} molecule was positioned exactly between two benzene rings of each ZnPc molecule, *not* at the center of ZnPc or ZnOEP molecule. The corrugation height of each bright spot measured from the molecular plane of ZnPc was approximately 0.45 nm, which is consistent with the value obtained for the supramolecular layer of C_{60} molecules from the 3-cyanophenyl-substited porphyrin layer on Ag(100), 0.44 nm, which was reported by Bonifazi and co-workers.[39] C_{60} molecules also can be seen at the "gap" sites between ZnPc molecules, indicating that the supramolecular assembly between ZnPc and C_{60} is stabilized by the C_{60} molecule trapped between ZnPc molecules in the bimolecular chessboard. This result indicates that the bimolecular chessboard makes it possible to form the supramolecular assembly of C_{60}, resulting in enhancement of subtle intermolecular interactions. As previously reported by Spillmann et al., the formation of the assembled C_{60} molecules was found on the porous network consisting of the cyanophenyl-substituted zinc porphyrin derivative formed on Ag(111) in UHV.[13] Each C_{60} molecule was located precisely on top of a porous porphyrin network, revealing that the selective inclusion of fullerene occurs within the hosting cavities arranged in a nanopatterned array. Thus, the bimolecular chessboard structure consisting of ZnPc and ZnOEP molecules is one of the building blocks of functional materials with tunable electronic and photophysical properties. It is noteworthy that the supramolecularly assembled C_{60} adlayer on the bimolecular chessboard is fairly stable at potentials where a structural change or the desorption of bimolecular chessboard structure is brought about by potential manipulation, although a potential dependence of the electronic structure of incorporated C_{60} molecules might be found when observations are made with greater care.

To explore further the effect of crystallographic orientation of the underlying Au on the bimolecular arrays composed of ZnPc and ZnOEP, the bimolecular adlayer on a reconstructed Au(100)−(hex) surface was examined in the same manner as described above. As shown in Figure 6, straight arrays consisting of ZnPc and ZnOEP molecules were found on the terrace. Even in the area of 75 × 75 nm^2 shown in Figure 6a, the surface was predominantly covered with alternate binary arrays composed of ZnPc and ZnOEP. As reported in our previous papers, this aspect is similar to that observed with the CoPc and CuTPP binary array on a reconstructed Au(100)−(hex) surface.[26b,26c] Several dark gaps were also observed on the terrace in the adlayer, suggesting that phase boundaries were formed as a result of lattice mismatch in the underlying Au atomic structure, i.e., these areas showed the (1 × 1) structure exposed by the lifting of reconstruction during the modification. Details of the internal structure, orientation, and packing arrangement of the binary ZnPc and ZnOEP adlayer on the Au(100)−(hex) surface are seen in Figure 6b, which is a close-up view of Figure 6a. In the area of 20 × 20 nm^2 shown in Figure 6b, it can be seen that alternate molecular rows are uniformly formed on the Au(100)−(hex) surface. Molecular chains of ZnOEP were clearly observed as slightly dark gaps between bright rows consisting

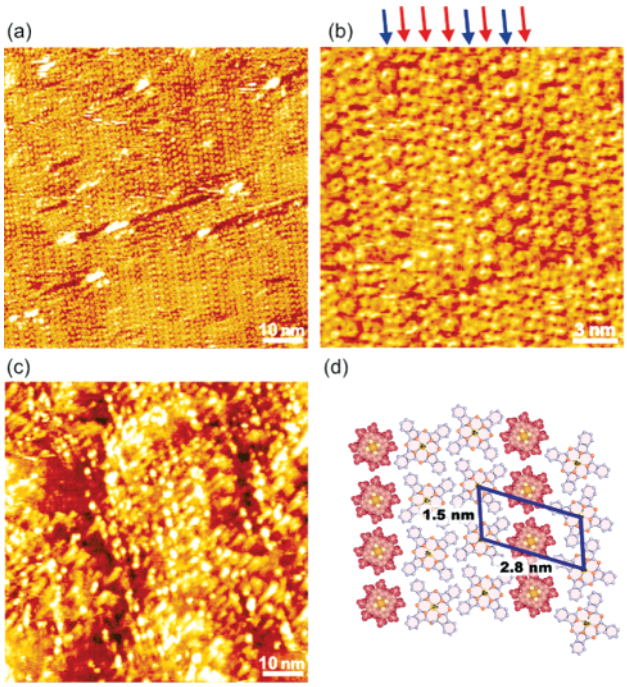

Figure 6. (a) Large-scale (75 × 75 nm^2) and (b) high-resolution (20 × 20 nm^2) STM images, obtained at 0.77 V vs RHE in 0.1 M $HClO_4$, of a bimolecular ZnPc and ZnOEP array formed on the reconstructed Au(100)−(hex) surface. Tip potential and tunneling current were 0.25 V vs RHE and 4.00 nA for both panels (a) and (b). (c) Typical STM image (75 × 75 nm^2), obtained at 0.60 V vs RHE in 0.1 M $HClO_4$, of C_{60} adlayer on the bimolecular ZnPc and ZnOEP array on Au(100)−(hex). Tip potential and tunneling current were 0.25 V vs RHE and 0.65 nA. (d) Proposed model of supramolecularly organized ZnPc and ZnOEP array on reconstructed Au(100)−(hex) surface.

of two or three rows of ZnPc molecules in Figure 6b. Each ZnPc molecule in the row marked by red arrows can be recognized as a propeller-shaped image with a central dark spot and four additional bright spots at the corners. These bright spots can be attributed to the benzene rings in the ZnPc molecule. One of four benzene rings in one ZnPc molecule fits into a "gap" in the neighboring ZnPc molecule. This kind of packing arrangement is found often in the single-component adlayer of ZnPc on Au(100)−(hex). On the contrary, individual ZnOEP molecules were found as a doughnut-shaped ring in the molecular row aligned along the direction indicated by blue arrows. Intermolecular distance between ZnPc (or ZnOEP) molecules in the molecular rows aligned in the direction indicated by the arrows was approximately 1.5 nm, which is consistent with the alternate array of ZnPc and ZnOEP induced by potential manipulation on Au(111). The shortest periodicity between ZnPc (or ZnOEP) molecular rows was approximately 2.8 nm (see the proposed model illustrated in Figure 6d). No gaps of bare Au surface were seen in the adlayer. Thus, the packing arrangement of the dominant bimolecular adlayer structure consisting of ZnPc and ZnOEP on Au(100)−(hex) was different from that obtained on Au(111). Although we could not observe the underlying Au atomic rows, the reconstructed atomic rows of Au(100)−(hex) are also likely to play a role as a molecular template, as shown in our previous papers.[26c,40] The bimolecular ZnPc and ZnOEP adlayer was stable in the potential range between 0.95 and 0.15 V.

(39) Bonifazi, D.; Spillmann, H.; Kiebele, A.; de Wild, M.; Seiler, P.; Cheng, F.; Jung, T.; Diederich, F. *Angew. Chem., Int. Ed.* **2004**, *43*, 4759.

(40) Yoshimoto, S.; Tada, A.; Suto, K.; Yau, S.-L.; Itaya, K. *Langmuir* **2004**, *20*, 3159.

After confirming the bimolecular adlayer on Au(100)−(hex), further adsorption of C_{60} was examined on the ZnPc and ZnOEP-modified surface. Figure 6c shows a typical STM image obtained after C_{60} adsorption. Unfortunately, no clear and regular patterns of individual C_{60} molecules are recognizable in the STM image. The average size of bright spots obtained in the STM image was approximately 2−3 nm, indicating that C_{60} molecules are aggregated with each other. This might be due to the difference in attractive interaction between the C_{60} molecules and the alternate bimolecular adlayer formed on the reconstructed Au(100)−(hex) surface. In the previous study on the electronic structure of C_{60} molecules on a reconstructed Au(100) surface obtained in UHV, it was reported that a strong chemical bond is formed between the C_{60} molecules and the Au substrate, as shown by ultraviolet photoemission spectroscopy and scanning tunneling spectroscopy experiments.[41] Actually, we have not yet succeeded in forming 1:1 supramolecular assembly of C_{60} on ZnOEP-modified Au(100)−(hex), whereas open-cage C_{60} derivative was found to form a 1:1 supramolecular assembled adlayer on the ZnOEP-modified Au(100)−(hex) surface.[31c] These results suggest that the attractive interaction of C_{60} molecules in the bimolecular array consisting of ZnPc and ZnOEP on the reconstructed Au(100)−(hex) surface is stronger than that on Au(111). To achieve a complete supramolecular assembly of C_{60} molecules on the bimolecular ZnPc and ZnOEP adlayer on Au(100)−(hex), much more careful attention should be paid to the modification conditions.

Conclusions

We succeeded in the formation of a uniquely nanostructured, bimolecular chessboard consisting of ZnPc and ZnOEP molecules and nanohexagon consisting of ZnTPP and ZnOEP. Our results show that bimolecular adlayers consisting of ZnPc and ZnOEP are controllable to generate various nanopatterns by precise electrode potential manipulation at the Au(111) surface, whereas the bimolecular ZnTPP and ZnOEP adlayer was independent of potential manipulation up to and near the hydrogen evolution potential. The electrochemical phase separation was caused by the difference in chemical structure, depending on the molecular packing arrangement of the bimolecular array.

We also demonstrated the formation of regular patterns of hybrid, supramolecularly assembled adlayers. The supramolecular assembly of C_{60} on the bimolecular chessboard on Au(111) yielded a regularly arranged fullerene nanodot pattern. The incorporation of C_{60} molecules into cavities in the bimolecular chessboard consisting of ZnPc and ZnOEP suggested the presence of a special electronic state. Thus, the chessboard structure consisting of ZnPc and ZnOEP plays an important role not only in the control of electron donating ability of the Au surface but also in the selective recognition of fullerene. A supramolecular organization of ZnPc and ZnOEP was also found on the reconstructed Au(100)−(hex) surface. The alternately arranged striped structure of ZnPc and ZnOEP was stable on the reconstructed Au(100)−(hex) surface. On the striped structure, it was difficult to find a regularly patterned supramolecular assembly of C_{60} molecules. The supramolecular assembly of C_{60} molecules was strongly influenced by the bimolecular packing arrangement of ZnPc and ZnOEP depending upon the crystallographic orientation of Au. The findings of this study provide a path toward the epitaxial growth of crystals on surface-supported supramolecular nanostructures to create a hybrid bilayer of supramolecularly assembled fullerenes, which will open wide applications to devices such as an optical switch.

Acknowledgment. This work was supported in part by CREST-JST, and by the Ministry of Education, Culture, Sports, Science and Technology, Grants-in-Aid for Young Scientists (B) (No. 16750106/18750132) and for the Center of Excellence (COE) Project, Giant Molecules and Complex Systems, 2007. S.Y. would like to express thanks to AIST for giving him the opportunity to carry out the additional experiments described in this article. The authors acknowledge the assistance provided by Dr. Y. Okinaka in writing this manuscript.

Supporting Information Available: Time-dependent STM images representing the bimolecular ZnPc and ZnOEP adlayer on Au(111) at 0.60 V vs RHE. Large-scale STM images of C_{60} arrays on the bimolecular chessboard at low and high coverage. This material is available free of charge via the Internet at http://pubs.acs.org.

JA077407P

(41) Kim, D. K; Suh, Y. D.; Park, K. H; Noh, H. P.; Kim, S. K.; Oh, J. S.; Kuk, Y. *J. Vac. Sci. Technol. A* **1993**, *11*, 1675.